REPORT DOCUMENTATION PAGE

Form Approved
OMB No. 0704-0188

PLEASE DO NOT RETURN YOUR FORM TO THE ABOVE ORGANIZATION.

1. REPORT DATE *(DD-MM-YYYY)*	2. REPORT TYPE	3. DATES COVERED *(From - To)*
07-17-2013	Conference Proceedings	

4. TITLE AND SUBTITLE

Sea Surface Signature of Tropical Cyclones Using Microwave Remote Sensing

5a. CONTRACT NUMBER

5b. GRANT NUMBER

5c. PROGRAM ELEMENT NUMBER

0601153N

6. AUTHOR(S)

Bumjun Kil, Derek Burrage, Joel Wesson and Stephan Howden

5d. PROJECT NUMBER

5e. TASK NUMBER

5f. WORK UNIT NUMBER

73-4260-03-5

7. PERFORMING ORGANIZATION NAME(S) AND ADDRESS(ES)

Naval Research Laboratory
Oceanography Division
Stennis Space Center, MS 39529-5004

8. PERFORMING ORGANIZATION REPORT NUMBER

NRL/PP/7330--13-1751

9. SPONSORING/MONITORING AGENCY NAME(S) AND ADDRESS(ES)

Office of Naval Research
One Liberty Center
875 North Randolph Street, Suite 1425
Arlington, VA 22203-1995

10. SPONSOR/MONITOR'S ACRONYM(S)

ONR

11. SPONSOR/MONITOR'S REPORT NUMBER(S)

12. DISTRIBUTION/AVAILABILITY STATEMENT

Approved for public release, distribution is unlimited.

13. SUPPLEMENTARY NOTES

14. ABSTRACT

Measuring the sea surface during tropical cyclones (TC) is challenging due to severe weather conditions that prevent shipboard measurements and clouds which mask the sea surface for visible satellite sensors. However, sea surface emission in the microwave L-band can penetrate rain and clouds and be measured from space. The European Space Agency (ESA) MIRAS L-band radiometer on the Soil Moisture and Ocean Salinity (SMOS) satellite enables a view of the sea surface from which the effects of tropical cyclones on sea surface emissivity can be measured. The emissivity at these frequencies is a function of sea surface salinity (SSS), sea surface temperature (SST), sea surface roughness, polarization, and angle of emission. If the latter four variables can be estimated, then models of the sea surface emissivity can be used to invert SSS from measured brightness temperature (T_B). Actual measured T_B from space also has affects due to the ionosphere and troposphere, which have to be compensated for, and components due to the galactic and cosmic background radiation those have to be removed. In this research, we study the relationships between retrieved SSS from MIRAS, and SST and precipitation collected by the NASA TMI sensor from the Tropical Rainfall Measuring Mission (TRMM) satellite during Hurricane Isaac, in August 2012. During the slower movement of the storm, just before landfall on the vicinity of the Louisiana Shelf, higher precipitation amounts were associated with lower SSS and slightly increased SST. This increased trend of SST and lower SSS under regions of high precipitation are indicative of inhibited vertical mixing. The SMOS Level 2 SSS were filtered by a stepwise process with removal of high uncertainty in T_B under conditions of strong surface roughness which are known to create noise. The signature of increased SST associated with increasing precipitation was associated with decreased SSS during the storm. Although further research is required, this study shows that there is a T_B signal from the sea surface beneath a tropical cyclone that provides information on roughness and salinity.

15. SUBJECT TERMS

microwave remote sensing, tropical cyclone, brightness temperature, sea surface salinity, precipitation

16. SECURITY CLASSIFICATION OF:			17. LIMITATION OF ABSTRACT	18. NUMBER OF PAGES	19a. NAME OF RESPONSIBLE PERSON
a. REPORT	b. ABSTRACT	c. THIS PAGE			Derek Burrage
Unclassified	Unclassified	Unclassified	UU	15	19b. TELEPHONE NUMBER *(Include area code)* (228) 688-5241

Reset

Standard Form 298 (Rev. 8/98)
Prescribed by ANSI Std. Z39.18

Sea surface signature of tropical cyclones using microwave remote sensing

Bumjun Kil[1]*, Derek Burrage[2], Joel Wesson[2] and Stephan Howden[1]
[1]Department of Marine Science in University of Southern Mississippi, Stennis Space Center, MS, USA
[2]Naval Research Laboratory, Oceanography Division, Stennis Space Center, MS, USA

ABSTRACT

Measuring the sea surface during tropical cyclones (TC) is challenging due to severe weather conditions that prevent shipboard measurements and clouds which mask the sea surface for visible satellite sensors. However, sea surface emission in the microwave L-band can penetrate rain and clouds and be measured from space. The European Space Agency (ESA) MIRAS L-band radiometer on the Soil Moisture and Ocean Salinity (SMOS) satellite enables a view of the sea surface from which the effects of tropical cyclones on sea surface emissivity can be measured. The emissivity at these frequencies is a function of sea surface salinity (SSS), sea surface temperature (SST), sea surface roughness, polarization, and angle of emission. If the latter four variables can be estimated, then models of the sea surface emissivity can be used to invert SSS from measured brightness temperature (T_B). Actual measured T_B from space also has affects due to the ionosphere and troposphere, which have to be compensated for, and components due to the galactic and cosmic background radiation those have to be removed. In this research, we study the relationships between retrieved SSS from MIRAS, and SST and precipitation collected by the NASA TMI sensor from the Tropical Rainfall Measuring Mission (TRMM) satellite during Hurricane Isaac, in August 2012. During the slower movement of the storm, just before landfall on the vicinity of the Louisiana Shelf, higher precipitation amounts were associated with lower SSS and slightly increased SST. This increased trend of SST and lower SSS under regions of high precipitation are indicative of inhibited vertical mixing. The SMOS Level 2 SSS were filtered by a stepwise process with removal of high uncertainty in T_B under conditions of strong surface roughness which are known to create noise. The signature of increased SST associated with increasing precipitation was associated with decreased SSS during the storm. Although further research is required, this study shows that there is a T_B signal from the sea surface beneath a tropical cyclone that provides information on roughness and salinity.

Keywords: microwave remote sensing, tropical cyclone, brightness temperature, sea surface salinity, precipitation

1. INTRODUCTION

Hurricane predictions have utilized measured sea surface temperature (SST) and wind speed, but sea surface salinity (SSS) has mainly been available only as model output. That is, the measurement of SSS has not been considered as an important factor. However, recent research shows that a thick layer of fresher-than-normal surface waters might affect the strength of a hurricane because it reduces mixing from deep water.[1] The heavy rainfall within hurricanes has the potential to freshen the sea surface and inhibit vertical mixing, and, thus, measurements of SSS within a hurricane, and after it passes, may be important for understanding hurricane evolution and lead to better prediction capabilities. SSS was shown as increased along a hurricane "wake" and that the increase could be explained by the hurricane eroding a barrier layer (a halocline within a thermocline).[4] However, it is shown that by adding rainfall to a model, the SSS was

Ocean Sensing and Monitoring V, edited by Weilin W. Hou, Robert A. Arnone, Proc. of SPIE Vol. 8724, 872413 · © 2013 SPIE · CCC code: 0277-786X/13/$18 · doi: 10.1117/12.2019112

reduced and vertical stability was increased up to two days after the passage of a storm.[3] Therefore, changes in SSS from pre-storm passage to during storm passage, related to precipitation within a hurricane, need to be studied to see the extent to which vertical mixing is enhanced by wind forcing or inhibited by rainfall. The heavy rainfall of Hurricane Isaac in 27-29 Aug. 2012 created extensive flooding in low lying areas of Louisiana. The total rain was reported as 6-13 inches[6], which exceeded that reported for Katrina as 5-10 inches[7]. In a preliminary study comparing SMOS SSS and modeled NOAA precipitation data, it was found that SSS was greatly reduced by the effect of rainfall during the near stationary movement of hurricane Isaac.[8] However, under hurricane conditions, SMOS SSS has an unknown bias due to uncertainties in the correction for surface roughness. Nevertheless, we hypothesize that we can find sea surface signatures consistent with barrier layer (BL) formation (i.e., low SSS and higher SST) by examining the regions where precipitation accumulation is greatest under a hurricane. In these regions, the decrease in SSS should be greatest, if vertical mixing is inhibited, and the signal to noise should be higher. There are four assumptions underlying the hypothesis: 1. The precipitation accumulation is greater underneath a slowly moving hurricane; 2. Vertical mixing is inhibited in these high accumulation regions and thus SSS has largest decreases; 3. SMOS SSS is precise enough under strong sea surface roughness conditions to accurately measure changes in SSS using an appropriate validation process. 4. The decreasing SSS represents inhibition of vertical mixing. 5. The signature of the BL can be presented as increased SST and decreased SSS during heavy rainfall.

2. DATA AND ANALYSIS

2.1 Microwave data set

The TRMM satellite is a research satellite designed to understand the distribution and variability of precipitation within the tropics as part of the water cycle in the current climate system. It provides much needed information on rainfall, SST, wind speed and water vapor in tropical cyclones. The information is retrieved from the multichannel passive microwave sensor called TRMM's Microwave Imager (TMI). The microwave sensor provides quantitative rainfall information covering an 878km wide swath on the sea surface. It works at five frequencies: 10.65, 19.35, 37.0, and 85.5 GHz at dual polarization and 22.235 GHz at single polarization. The TMI swath covered hurricane Isaac off the Louisiana coast during overflights on both the 27 and 28 Aug. 2012. The Soil Moisture and Ocean Salinity (SMOS) satellite of the European Space Agency (ESA) was launched in November 2009 and is the first satellite designed to measure soil moisture and ocean salinity using an interferometric L-band (21 cm, 1.4 GHz) Microwave Imaging Radiometer using Aperture Synthesis (MIRAS). It was deployed at an altitude of 758 km with a dusk-dawn sun-synchronous orbit with an inclination of 98.44^{0}.[9,10,11,12] The orbit repeats every 23 days, but every 3 days it approximately repeats. L-band radiation is not absorbed by clouds, which makes it possible to retrieve SSS in bad weather conditions. The SSS retrieval is dependent upon sea surface roughness, SST, polarization, viewing angle, and corrections for sun glint, galactic and cosmic background radiation, and Stokes effects of the ionosphere. The accuracy of a given retrieval can be improved by averaging in time and space. In the tropics, where the warm SSTs result in a higher signal to noise ratio, a 10 day averaged SSS SMOS product is ~ 0.3 psu.[13] It is well known that fresh water lenses, originated by rainfall, have been measured by SMOS in tropical regions.[14,22] In those studies the surface freshening rate was estimated at about -0.2 psu per 1 mm/hr. [14,22] However, these results were found under moderate surface conditions, not on TC conditions. For TC conditions although the roughness algorithms are not as accurate the precision may be good enough to accurately measure SSS changes during a hurricane. In this research, surface precipitation and SST data were used from the TRMM satellite. The SMOS Level 2 (L2) dataset includes not only SSS, but also ECMWF wind speed which is used for the estimates of sea surface roughness on emissivity. To estimate the difference between Tropical cyclones passing through the region and before, the date prior to TC is set up as 23 Aug 2012 which has both SMOS and TRMM data in common.

2.2 Study area and analysis

The study area is the eastern Gulf of Mexico that was impacted by hurricane Isaac. After Isaac moved past the west coast of Florida and towards the northern Gulf coast, it slowed down considerably. In this latter region the slow propagation speed resulted in higher precipitation accumulation amounts. Areas of the sea surface directly impacted by Isaac, which showed increases of SST relative to pre-storm values (TMI ΔSST >0) were selected for analysis since this indicates lower vertical mixing. It is important to note that ΔSST was only able to be computed where TMI swaths during the hurricane and before the hurricane overlapped. The nearest, in space and time SMOS data (pre-storm and during storm) were then analyzed to determine if appreciable freshening also occurred. We selected portions of the two different microwave satellite data sets, and relevant auxiliary data sets, by the following criteria. First precipitation and SST from TMI were selected if SST increased under the hurricane. Next SSS from SMOS, and associated ECMWF winds, were chosen closest in time and space to the selected TMI measurements (pre-storm and during-storm). As a next stage, ΔSSS was computed and compared with precipitation to see if there was a consistency with freshening by rain fall.

Table 1. TMI data set for selecting study region (West FL: West Coast of Florida, GCR : Gulf Coast Region)

Satellite	Sensor	Freq.	Swath date and time	Focusing Area	NOAA TC Location (Speed of TC Center movement)	Used data
TRMM	TMI	10.7GHz	23:55 UTC in 22 Aug. – 01:27 UTC in 23 Aug. 2012	West FL, GCR	-	SST (deg C), Precipitation (mm/hr)
			21:50 UTC in 26 Aug. – 23:22 UTC in 26 Aug. 2012	West FL	West FL (16 mph)	
			20:56 UTC in 27 Aug. – 22:28 UTC in 27 Aug. 2012	GCR	GCR (12 mph)	
			03:05 UTC in 28 Aug. – 04:37 UTC in 28 Aug. 2012	GCR	GCR (10 mph)	

The TMI data just before Isaac entered the Gulf was on August 22, and the first data after Isaac entered the Gulf was on August 26 (Table 1). The ΔSST, for the overlapping segments of the two swaths, showed overall cooling off the west coast of Florida (Figure 1) as the storm propagated relatively rapidly at 16 mph. Later, when Isaac moved into the northern Gulf coast region and slowed appreciably to 10 mph, the SST difference between TMI measurements from passes over the storm on 28 August and 27 August and measurements before the storm on 23 August there were areas on positive values (as high as 1.16^{o}C and 0.85^{o}C, respectively) close to the regions of high precipitation (Figure 1). The close correspondence between positive SST changes and precipitation leads to questions about the potential role sea surface freshening may play in this phenomenon. In a recent study related with Hurricane Katia, SST under the hurricane was found to be increased around the Amazon River plume, however preexisting barrier layers were shown to play a role.[4] The Gulf Coast region also has major river discharge similar to the Amazon River, but the observations shown here for Isaac are well offshore.

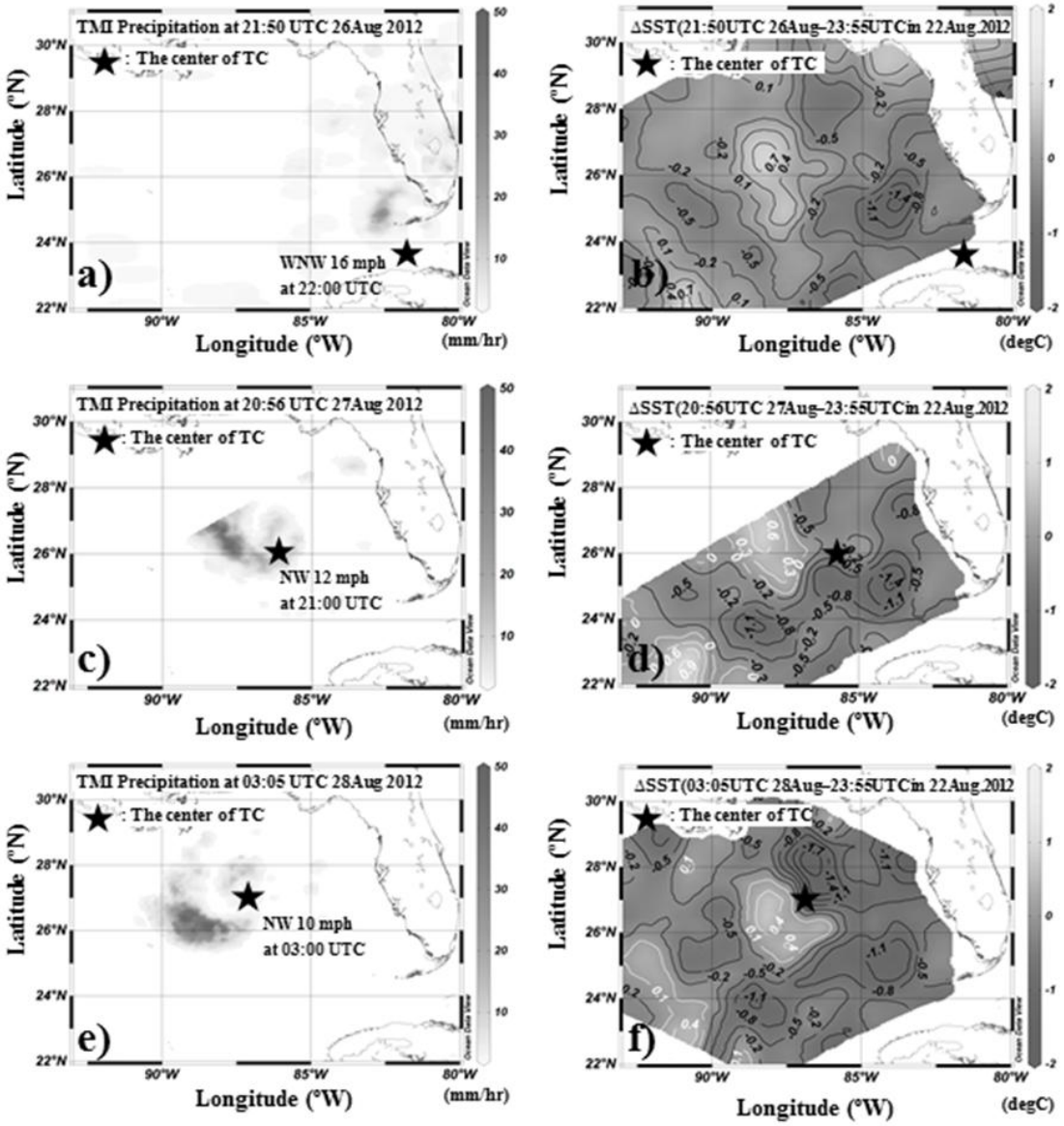

Figure 1. Horizontal distribution of precipitation: a), c), e) and ΔSST (during storm – pre-storm): b),d),f)

3. RESULTS

3.1 The validation process for the SMOS data

The SMOS L2 tracks in the Gulf Coast region from 11:06-12:00 UTC on 23 Aug.2012 and 11:12-12:05 UTC on 28 Aug.2012 were selected as closest in time and location to the selected TMI ΔSST and precipitation data (Table 2). Coincidently, the track on 28 Aug.2012 not only includes the center of Isaac but also has a fair amount of time separation from 23 August track; thus, it is applicable for comparing moderate sea surface condition along with TMI data in the Gulf Coast region on 23 Aug.2012.

Table 2. The Satellite data set for the analysis in the Gulf Coast region

Satellite	Swath date and time	Used data
TRMM	23:55 UTC in 22 Aug. – 01:27 UTC in 23 Aug. 2012	SST (deg C), Precipitation (mm/hr)
	20:56 UTC in 27 Aug. – 22:28 UTC in 27 Aug. 2012	
	03:05 UTC in 28 Aug. – 04:37 UTC in 28 Aug. 2012	
SMOS	11:06 UTC in 23 Aug. – 12:00 UTC in 23 Aug. 2012	SSS (psu), ECMWF Wind Speed (m/sec) (Auxiliary data)
	11:12 UTC in 28 Aug. – 12:05 UTC in 28 Aug. 2012	

Careful consideration needs to be made for using SMOS SSS retrieved from a sea surface under hurricane conditions. In particular the roughness correction to the sea surface emissivity is suspect under these conditions. Sea surface roughness increases the emissivity which in turn increases T_B in both V, H polarization at most incident angles.[17,20] Insofar as sea surface roughness is a well-defined function of wind speed, an empirically based correction can be made. Special care was taken to minimize other error sources in the SMOS data. Applied Research in Geomatics, Atmosphere, Nature & Space (ARGANS) recommends a threshold parameter for filtering L2 data based upon a parameter, which represents the overall quality assessment for retrieving SSS.[16,17] The index is based upon the quadratic sum of all error contributions such as galactic noise, RFI contamination, radiometric noise and other uncertainties. If the index is 999 or more, the data has not been processed and is generally not used. However applying the existing ARGANS's recommendations enormously diminishes the dataset within the tropical cyclone region. Therefore a different method was used that considered specific parameters in the SMOS L2 data. First, the degradation of T_B can be parameterized as uncertainty (sigma) in independent polarization. This parameter is also known to the sensitivity to wind speed.[16,17] Due to strong wind, the sensitivity of T_B to the sea surface roughness is amplified in h and v polarization in most incidence angles.[17] The uncertainty of the T_B sensitivity to wind speed is on the order of 0.1 K per 1 m/sec for all incidence angles.[19] Considering the T_B sensitivity to SSS (0.35 - 0.8 K/psu at V-pol, and 0.2 - 0.6 K/psu)[17], it is presumable that wind speed at 20 m/sec in severe sea surface roughness conditions can be translated into a T_B uncertainty of 2 K and ΔSSS of 2.4 - 10 psu. Second, there are three options for retieved SSS that utilize three different roughness correction models. In this study, stepwise validation is performed using procedures considering the specific parameters shown in figure 2. The first step is selecting the SSS model (i.e., roughness model), filtering out data contaminated with RFI and galactic noise, and adjusting the acceptable range from the center of the swath to -300/+300 km as recommended by ARGANS.[16,18] The parameter called number of valid measurements available for retrieval (Dg_num_meas_valid) was employed for adjusting the acceptable range based upon different amounts depending on incident angle. The galactic noise was filtered using the parameter called the number of measurements discarded due to errors in galactic noise (Dg_galatic_Noise_Error). The removal of RFI contamination was done using the parameter termed number of measurements suspected of being contaminated by RFI (Dg_RFI_L2) and number of measurements available in L1c product (Dg_num_meas_L1C) to estimate the RFI probability (100* Dg_RFI_L2/ Dg_num_meas_L1C).[16] The second step is to eliminate the data having a high uncertainty for T_B and which appears distributed unusually offset compared with a normal Gaussian PDF (Probability Density Function) plot.

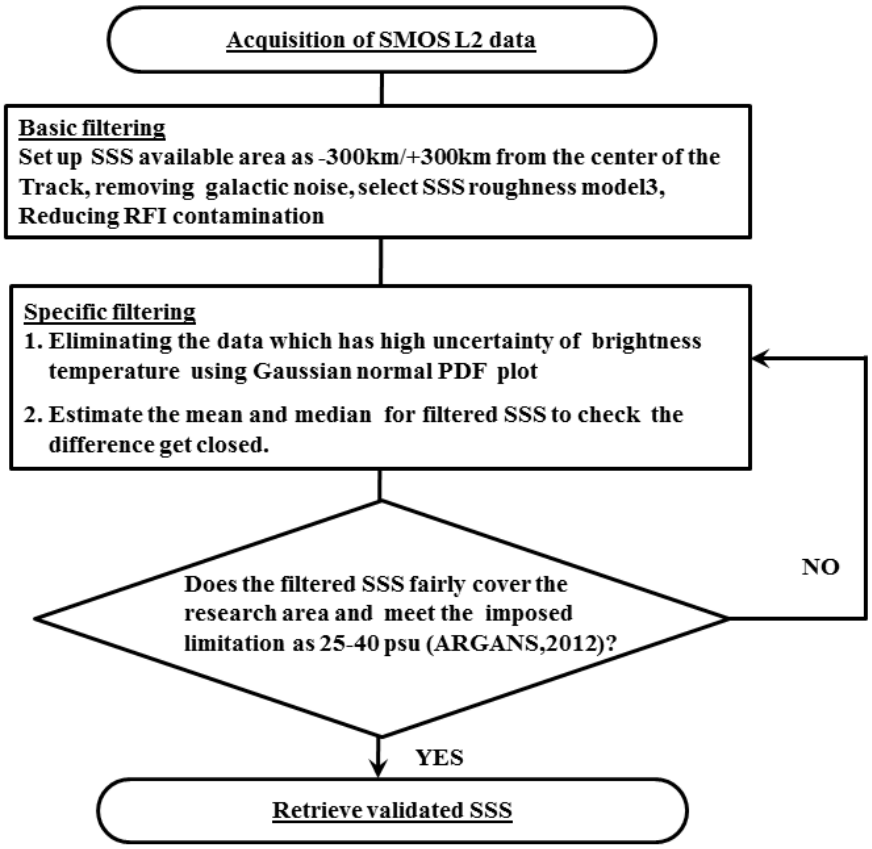

Figure 2. The algorithm of stepwise validation process

Finally, the difference between the mean and median of the validated SSS, compared with the pre-filtered version, is used to check the improvement and evaluate that the validated SSS range lies within the limited SSS range imposed by ARGANS[16]. If the validated SSS range still has values over the the upper or lower threshold, or an unusual offset comparing with normal PDF plot, then the process is to revert to step 2 and tighten the threshold on the T_B uncertainty. The initial choices of parameters to use in the various filtering steps are listed in Table 3. The SSS that used roughness model 3 (i.e., SSS3) was selected because it is known as applicable for various surface conditions with relatively low bias compared with other models.[15] Galactic noise error was eliminated as 25 % in 23 Aug. and 15 % in 28 Aug.2012. RFI contamination was removed by retaining the probabilities less than 33% as recommended by ARGANS. Although the data was filtered to 40-42% in the first step, the uncertainty of T_B was still shown to be offset within 10 % of the data as shown in the figure 3. Therefore, as a second step, the uncertainty which showed T_B (H) > 0.75 K , T_B (V) > 0.9K in 23 Aug.2012 and T_B (H) > 1.8 K , T_B (V) > 0.9K in 28 Aug.2012 were empirically eliminated for comparing with the normal PDF plot. Consequently, the data which has high T_B uncertainty as 2.6% in 23 Aug.2012 and 3.5% in 28 Aug. 2012 was removed.

Table3. The criteria for the basic filtering as a first step

File Name	Number of filtered data due to galactic noise error	Acceptable range from the center of the track	Number of valid measurement available for SSS retrieval	SSS retrieval model Selection	RFI (%)	Selected Section	The number of Filtered data (sampled % from total raw data)
MIR_OSUDP2_20120823T110645 _20120823T120004_550_001.zip (Before storm)	28797(22%) → 0	-300 ~ +300km	> 150	RM3	< 33%	Lon.:93-84W Lat.:22-31N	55511(42%)
MIR_OSUDP2_20120828T111207 _20120828T120526_550_001.zip (During storm)	16039(14%) → 0						47110(40%)

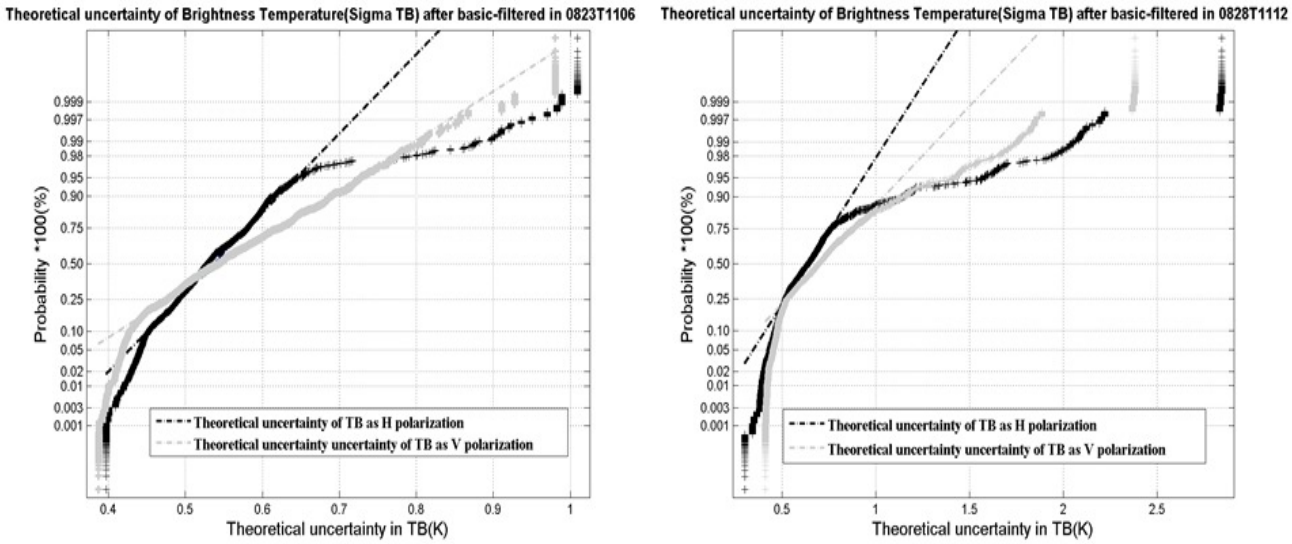

Figure 3. The SMOS uncertainty of T_B in H(black) and V(gray) polarization with normal PDF plot in a) 23 Aug. 2012 b) 28 Aug. 2012 prior to the second step.

As a result of stepwise validation, the data from each track was finally retrieved as 41.5% in 23 Aug.2012, 39 % in 28 Aug.2012 and the SSS range was shortened to 29.64 - 38.8 psu in 23 Aug. and 28.69 – 38.72 psu in 28 Aug.2012 as shown in table 4. Each validated SSS (black) successfully fulfills the imposed limitation defined by ARGARNS[16] despite the remaining outliers from the recommended threshold of 31-37 psu (see comparison with pre-validated SSS (gray) in figure 4). Although the data still outliers from the recommended threshold, the mean and median of each data set show fairly closed to the values when filtering by quality index. The lowest part of SSS still shows offset pattern from normal PDF plot but this offset might have originated from the coastal environment such as river discharge or heavy rainfall. Although the validation still has a caveat related with threshold, it should be acceptable as far as the threshold does not include the Gulf Coast region.

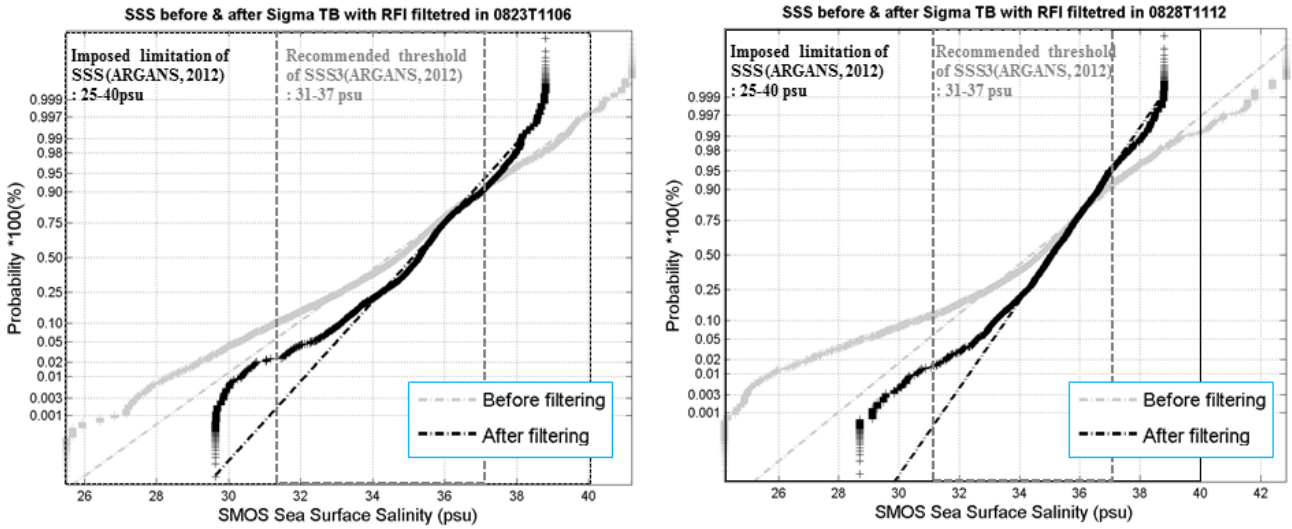

Figure 4. The SMOS pre (gray) and post (black) validation, SSS comparing with normal PDF plot as a) 23 Aug. 2012 b) 28 Aug. 2012. Red

Table 4. Comparison of SSS resultes from validation methodologies in 23, 28 Aug.2012

	Validation	Mean	Median	Max.	Min.	Max. uncertainty of SSS	N
MIR_OSUDP2_20120823T110645 _20120823T120004_550_001.zip	Before	34.39	34.70	41.19	25.49	2.05	130268
	Stepwise validation	**35.09**	**35.29**	**38.80**	**29.64**	**0.93**	**54038 (41.5%)**
	ARGANS	**34.95**	**35.34**	**38.69**	**29.64**	**0.86**	**22384 (17%)**
MIR_OSUDP2_20120828T111207 _20120828T120526_550_001.zip	Before	34.19	34.7	42.84	24.19	2.67	117604
	Stepwise validation	**34.95**	**35.08**	**38.72**	**28.69**	**0.99**	**45429 (39%)**
	ARGANS	**35.07**	**35.23**	**38.72**	**29.93**	**1.17**	**15112 (13%)**

3.2 Precipitation and Inhibition of Vertical Mixing

The ΔSSS (values during tropical storm minus pre-storm: 11:12 UTC in 28 Aug.2012 - SSS at 11:06 UTC in 23 Aug.2012) are shown as horizontal distributions and in histogram form in figure 5. In the histogram, a negative bias (white color shading in Fig.5d) was dominant in the mean and median probably due to heavy rainfall during the TC. Despite the strip removed due to galactic noise, each distribution was useful for estimating horizontal ΔSSS near TC in the Gulf Coast region. When superimposing SMOS SSS and ECMWF wind speed with TMI SST and precipitation in

one panel in figure 6, the depression of SSS seems to show the signature of precipitation, due to slow movement of TC. In addition, the positive ΔSST was observed near the center of the SSS low at 26 ºN. Thus, it suggests the usefulness of ΔSSS as an indicator of precipitation. Secondarily, the positive ΔSST found in the same region is indicative of inhibited vertical mixing as that would increase SSS and decrease SST. Thus, the relation between wind speed and ΔSSS under the TC was depicted along with precipitation using a 3D axis plot in figure 7. The data were plotted based upon wind speed > 12 m/sec, and precipitation 2 mm/hr. On the relation between wind speed and ΔSSS in figure 7a), the ΔSSS seems to decrease with increasing wind speed at a slope around 0.154 psu per 1 m/sec, but it does not show a significant correlation due to small r-squared values. Besides, the standard deviation shows high uncertainty for increasing wind speed.

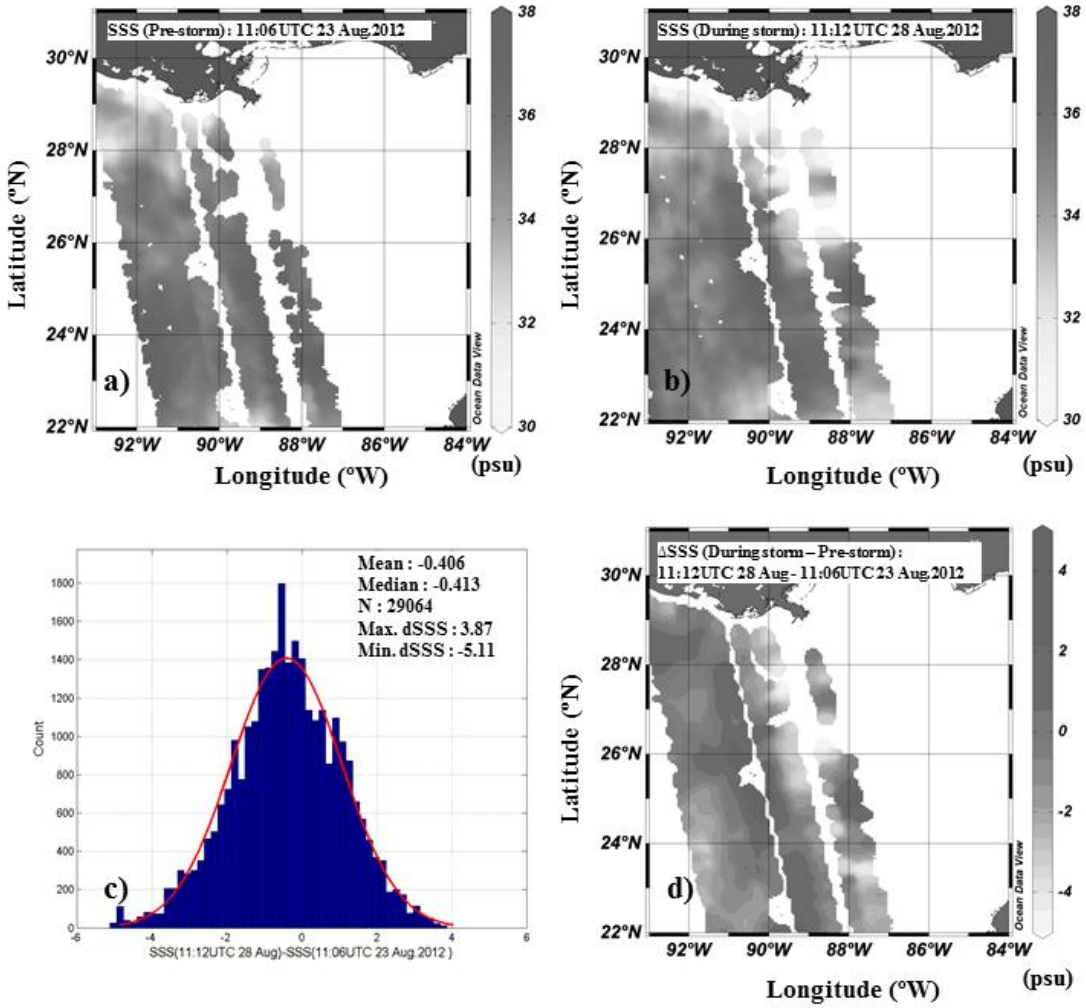

Figure 5. The distribution of validated SSS in a) 23 Aug. 2012 b) 28 Aug. 2012.The differences of SSS in 28 – 23Aug. 2012 (ΔSSS) are on c) Histogram d) Horizontal distribution.

Several peaks of precipitation are located near regions of low ΔSSS and high wind speed position, which suggests the effect of intense rainfall in decreasing SSS within the TC. The relation between wind, precipitation and ΔSSS in figure 7b), however, has a slope of 0.079 psu per 1 mm/hr, with better correlated r-squared values around 0.24 under widely distributed wind speeds up to 20 m/sec. Accordingly, we can estimate the drop of SSS around 0.8 psu per 10 mm/hr within the TC.

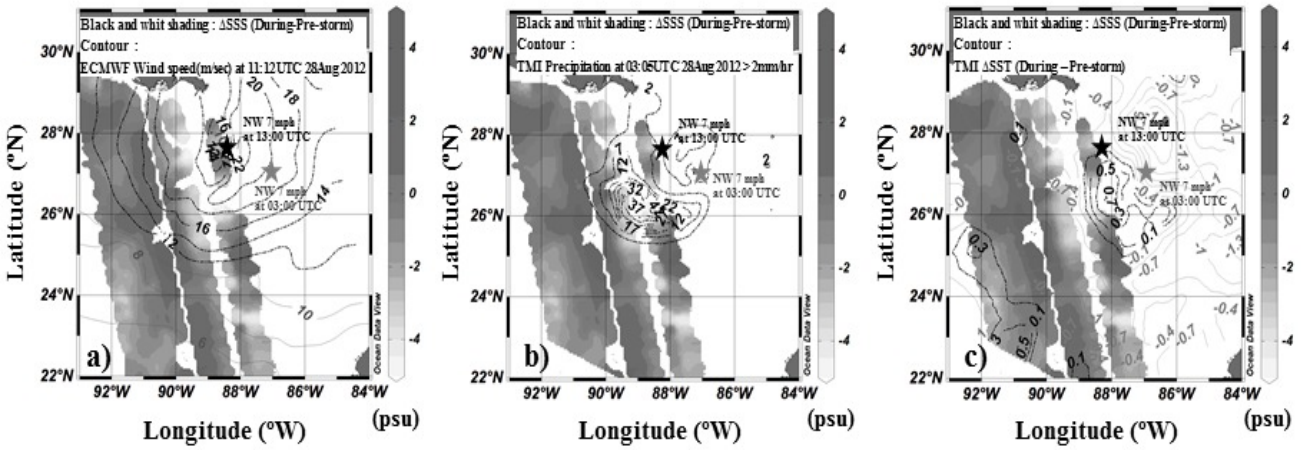

Figure 6. The horizontal distribution of ΔSSS super positioned with the contour line as a) ECMWF wind speed b) TMI precipitation c) TMI ΔSST. The gray star: the center of TC closed in TMI L2 track, black star: the center of TC closed in SMOS L2 track, which is based on NOAA National Hurricane Center.[23] TMI data: 03:05 UTC in 28 Aug.2012, SMOS data: 11:12 UTC in 28 Aug.2012.

The negative ΔSSS peak with value close to -5.5 psu that is approximately collocated in a region of light precipitation might be explained, considering the movement of theTC, as due to a previous intense freshening several hours prior. Therefore, heavy rainfall within the TC appears to result in inhibited vertical mixing.

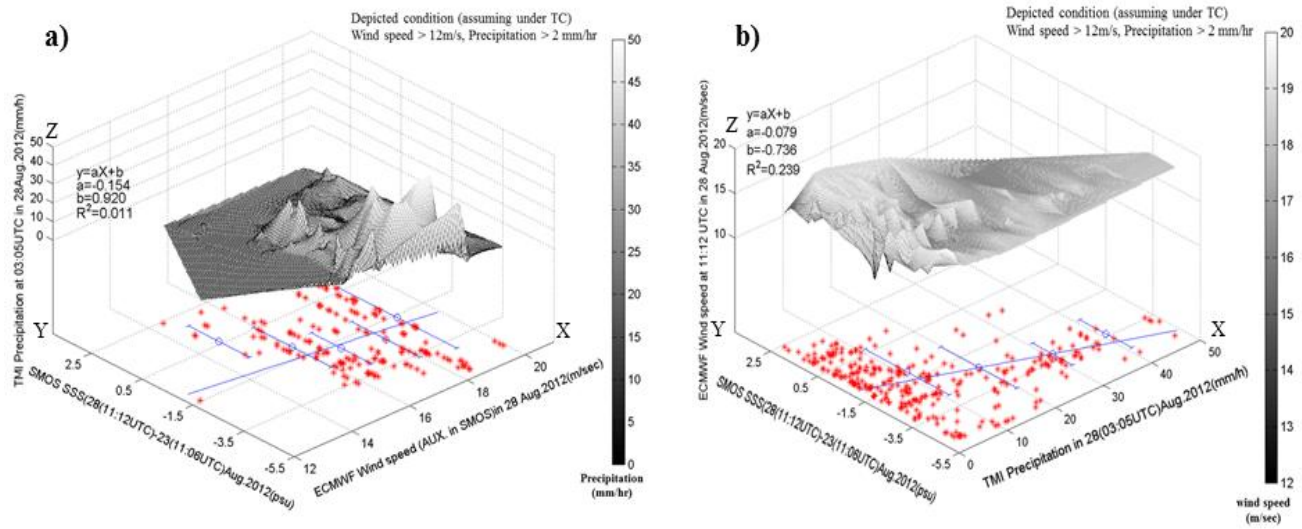

Figure 7. 3D axis plot as a) X: ECMWF wind speed, Y: ΔSSS and Z: precipitation b) X: Precipitation, Y: ΔSSS and Z: ECMWF wind speed. The plot is presented on the bases of TC condition (precipitation : > 2mm/hr, wind speed >10m/sec) at 03:05 UTC in 28 Aug.2012

To further see the effects of inhibited vertical mixing during heavy rainfall, we sampled the TMI data which is independently located closest to negative SMOS ΔSSS data within a 6NM radius on 27, 28 Aug.2012. To see the accumulated precipitation effect into ΔSST, we relate the precipitation in 27 Aug.2012 to ΔSST in 28 Aug.2012 as well. Each selected TMI data point is sampled based on TC conditions (winds speed > 12 m/sec, ΔSSS < 0, precipitation > 2 mm/hr) and gets merged with SMOS ΔSSS and ECMWF wind speed based upon TMI location as shown in superimposed distribution in table 5. As a result of merging, we sampled 35-231 counts for 27, 28Aug. 2012.

Table 5. Merged data (SMOS+TMI) on the basis of TC conditions on the separate date of precipitation as 27, 28Aug.2012.

Data set (TMI+SMOS)	Sampling criteria bases on TC			Range of sampled ΔSST (degC)	n	Merging radius
	Wind speed (ECMFW AUX in SMOS)	Precipitation in TMI	ΔSSS			
• ΔSSS at 11:12UTC in 28Aug. 2012 • ΔSST (28-22Aug.) vs precipitation at 03:05UTC in 28Aug. 2012	>12 m/sec	> 2 mm/hr	< 0	-0.85 – 0.53	231	< 6NM
• ΔSSS at 11:12UTC in 28Aug. 2012 • ΔSST (28-22 Aug.) vs precipitation at 20:56UTC in 27Aug. 2012				-1.2 – 0.5	54	

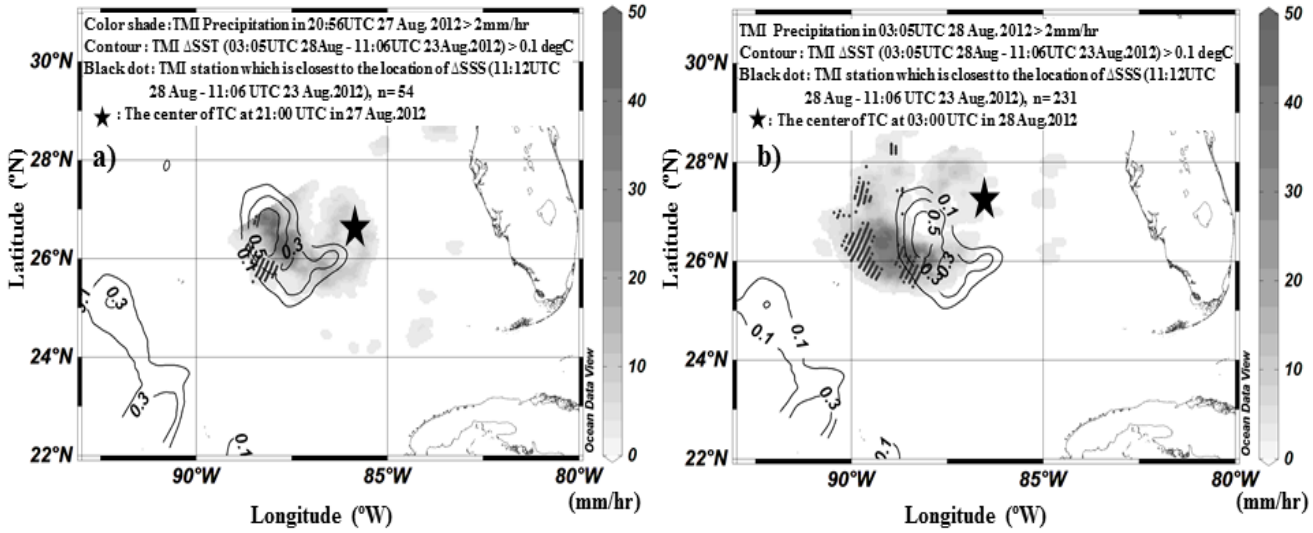

Figure 8.The horizontal distribution of a) Precipitation 27Aug.2012 and ΔSST in 28Aug.2012. b) Precipitation and ΔSST in 27Aug.2012.The contour line is ΔSST > 0.1 degC and the black dot is the sampled TMI data which has TMI precipitation, ΔSST, SMOS ΔSSS and ECMWF wind speed.

Unfortunately, the subsampled data for 27 Aug.2012 has much fewer TMI data than that from 28 Aug. due to the limited distribution of SMOS data close to TMI data. Superimposing ΔSST with precipitation shows that the peak of ΔSST in 28Aug. has a very similar shape with the precipitation distributed for 27 Aug. (Figure 8). Assuming a lasting freshening stratified condition, and inhibition of vertical mixing, the ΔSST for 28 Aug. is probably related to the intense precipitation which accumulated for more than 6 hours. Using the selected data, specifically, we display the relations between ΔSST and precipitation in terms of reduced amount of SSS (abs (ΔSSS)) dependence as a 3D axis plot as shown in figure 9. In the relation for Fig. 8a) on 27Aug.2012, the slope was positive but had small r-squared values probably due to the small amount of freshening as shown in the figure 9a). When freshening of > 3.8 psu was used as a criteria, both the slope and r-squared values increased to 0.011 degC per 1 mm/hr and 0.348 as shown in figure 9b). The patterns shown in Fig.8b) are similar to the pattern in Figure 9c), d) as well. To put this in another way, the slope can be expressed as 0.11 degC per 10 mm/hr in accumulated heavy rainfall near the center.

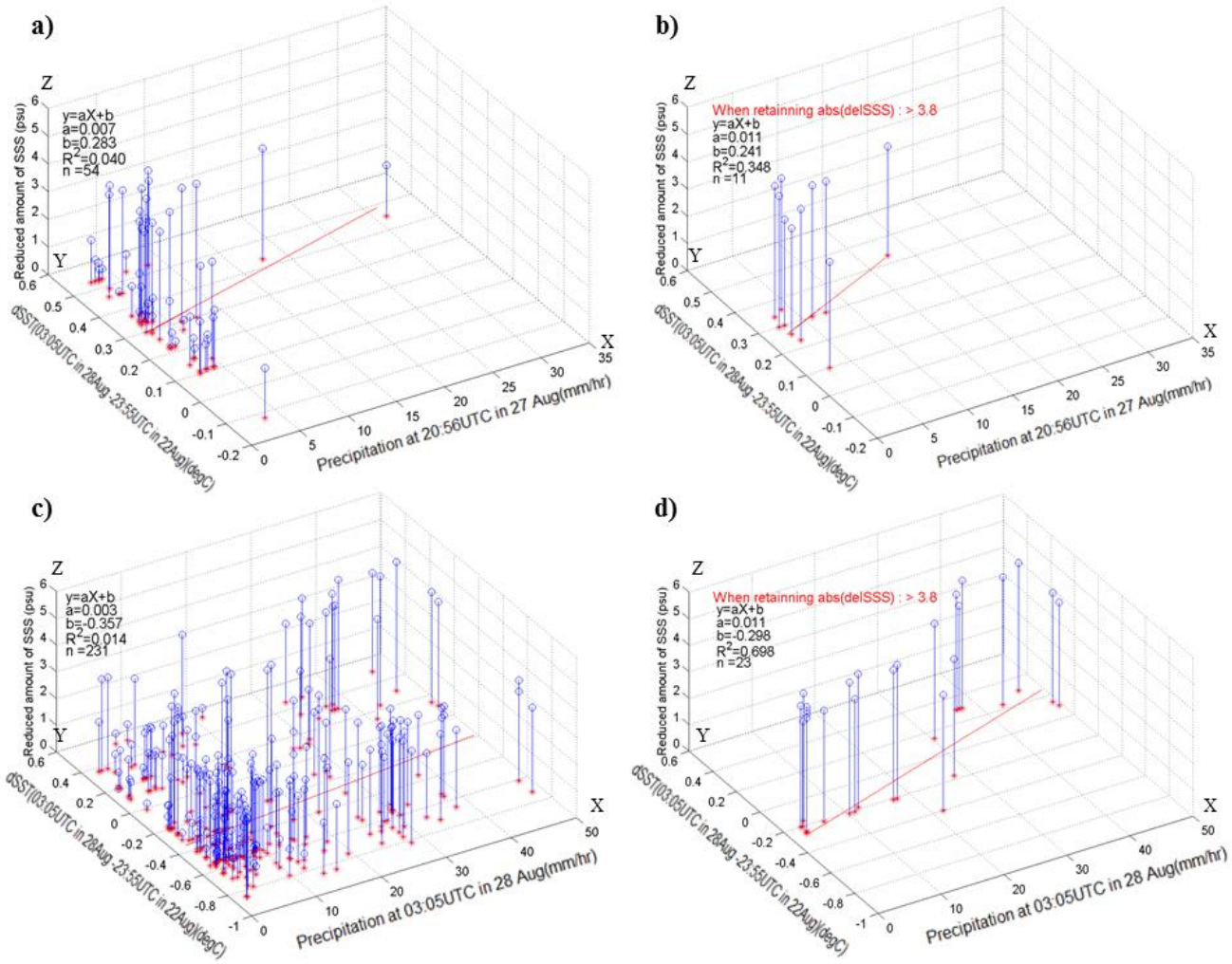

Figure 9. The 3D axis stem-plot (X: precipitation, Y: ΔSST, Z: abs (ΔSSS)) the pre-filtered ΔSSS as a) Fig. 8a) , c) Fig. 8b), and post-filtered ΔSSS as b) for Fig. 8a) , d) for Fig. 8b) in terms of abs (ΔSSS)) > 3.8 psu

When we controlled the abs (ΔSSS) incrementally in more detail, as in table 6, both slope and r-squared values tended to increase gradually so that the SST probably increased with intense freshening. This trend supports that the heavy precipitation can result in inhibited vertical mixing.[1] Thus, the connection of rainfall and ΔSST within a TC requires further research to see if there is an affect on intensity and/or track.

Table 6. The table of the slope, R^2 and N for each linear regression plot with incremental filtering of ΔSSS

Reduced amount of SSS (psu)	ΔSST (28-22 Aug.) vs Precipitation at 20:56UTC in 27Aug. 2012			ΔSST (28-22Aug.) vs Precipitation at 03:05 UTC in 28Aug. 2012		
	a (degC/mm/hr)	R^2	n	a (degC/mm/hr)	R^2	n
abs (ΔSSS) > 0	0.007	0.04	54	0.003	0.014	231
abs (ΔSSS) > 2.1	0.009	0.093	22	0.006	0.089	125
abs (ΔSSS) > 3.8	0.011	0.35	11	0.011	0.698	23

4. CONCLUSION/SUMMARY

Tropical storm Isaac provided conditions indicating low vertical mixing during near stationary movement with intense rainfall when it passed through the Gulf Coast region. These results are still preliminary as further examination of both the uncertainties in TMI and SMOS data within strong wind conditions is needed. For the SMOS satellite data, initially, the correction of the contamination which is induced by coastal environmental condition such as strong sea surface roughness/RFI and land contamination is necessary. A stepwise validation was attempted to retrieve the SSS when TC Isaac went through the Gulf Coast region by statistically and stepwise filtering the uncertainty of T_B. The SSS in pre-storm condition in 23 Aug. 2012 was also validated to estimate the difference between pre-storm and during the storm. The validated SSS, as a result, showed improved quality and provided a larger amount of coverage compared with the usual filtering criteria. A distinctly low ΔSSS was observed, as low as -5.1 psu, near the center of the TC associated with heavy rainfall, as high as 50 mm/hr, with a freshening tendency of -0.79 psu per 10 mm/hr. The relation between precipitation and ΔSST for pre-storm and during storm conditions was shown to be positive with values of 0.06 – 0.11 degC per 10 mm/hr associated with a negative ΔSSS.

REFERENCE

[1] K. Balaguru, P.Chang, R. Saravanan, L. Ruby Leung, Z. Xu, M. Li and J.S. Hsieh, "Ocean barrier layers' effect on tropical cyclone intensification," PNAS **109**(36), 14343-14347 (2012).

[2] S. D. Jacob and C. J. Koblinsky, "Effects of Precipitation on the Upper-Ocean Response to a Hurricane," American Meteorological Society **135**, 2207-2225 DOI: 10.1175/MWR3366.1(2007).

[3] Mignot, J., A. Lazar, and M. Lacarra," On the formation of barrier layers and associated vertical temperature inversions: A focus on the northwestern tropical Atlantic," *J. Geoph.Res.*, **117**, C02010 (2012), doi:10.1029/2011JC007435.

[4] Grodsky, S. A., N. Reul, G. S. E. Lagerloef, G. Reverdin, J. A. Carton, B. Chapron, Y. Quilfen, V. N. Kudryavtsev, and H.-Y. Kao,"Haline hurricane wake in the Amazon/Orinoco plume: AQUARIUS/SACD and SMOS observations," Geophys. Res. Lett., doi:10.1029 /2012GL053335 (2012).

[5] Pailler, K., B. Bourlès, and Y. Gouriou, "The barrier layer in the western tropical Atlantic Ocean," *Geoph. Res. Lett.*, **26**, 2069–2072 (1999).

[6] NASA, "Hurricanes/Tropical Cyclones," 6 Sep. 2012, http://www.nasa.gov/mission_pages/hurricanes/archives/2012/h2012_Isaac.html.

[7] NASA, "Hurricanes/Tropical Cyclones,"24 Aug. 2005,http://www.nasa.gov/mission_pages/hurricanes/archives/2005/h2005_katrina.html.

[8] Kil,B., Burrage, D., Wesson, J., and Howden, S., "Monitoring sea surface salinity changes near the Gulf Coast during Hurricane Isaac using microwave remote sensing," Proc.Bays&Bayous Conference, Biloxi, Mississippi, November 14-15 (2012).

[9] Y. H. Kerr, P. Waldteufel, J. P. Wigneron, J. Font, and M. Berger, "The objectives and rationale of the Soil Moisture and Ocean Salinity (SMOS) mission," Proc. IGARSS-Scanning the Present and Resolving the Future **1**(7), 1004–1006 (2001).

[10] Y. H. Kerr and D. M. Le Vine, "Foreword to the special issue on the Soil Moisture and Ocean Salinity (SMOS)mission," IEEE Trans. Geosci. Remote Sens. **46**(3),583–585(2008).

[11] Y. H. Kerr, P. Waldteufel, J. P. Wigneron, S. Delwart, F. Cabot, J. Boutin, M. J. Escorihuela, J. Font, N. Reul, C. Gruhier, S. E. Juglea, M. R. Drinkwater, A. Hahne, M. Martin-Neira, and S. Mecklenburg, "The SMOS mission: New tool for monitoring key elements of the global water cycle," Proc. IEEE **98**(5), 666–687(2010).

[12] J. Font, A. Camps, A. Borges, M. Martin-Neira, J. Boutin, N. Reul, Y. H. Kerr, A. Hahne, and S. Mecklenburg, "SMOS: The challenging sea surface salinity measurement from space," Proc. IEEE **98**(5), 649–665 (2010).

[13] Reul, N., J. Tenerelli, J. Boutin,; B. Chapron, F. Paul, E. Brion, F. Gaillard, and O. Archer,"Overview of the first SMOS sea surface salinity products. Part I: quality assessment for the second half of 2010," IEEE Trans. Geosci. Rem. Sens., **50**, 1636-1647(2012a).

[14] Hénocq, C., Boutin, J., Reverdin, G., Petitcolin, F., Arnault, S.,and Lattes, P.," Vertical Variability of Near-Surface Salinityin the Tropics: Consequences for L-Band Radiometer Cali-bration and Validation," J. Atmos. Ocean. Tech., **27**, 192–209,doi:10.1175/2009jtecho670.1(2010).

[15] Boutin, J., Martin, N., Yin, X., Font, J., Reul, N., Spurgeon, P., "First Assessment of SMOS Data Over Open Ocean: Part II-Sea Surface Salinity" IEEE Trans. Geosci. Remote Sens. 50,1662-1675(2012).

[16] ARGANS, "SMOS L2 OS Product Performance Status Report," Doc:SO-PR-ARG-GS-0056, November 30(2012).

[17] ARGANS, "SMOS L2 OS Algorithm Theoretical Baseline Document," Doc: SO-TN-ARG-GS-0007, June 9 (2010).

[18] The SMOS L2 OS Team, "Read-me-first note for SMOS level 2 Ocean Salinity data products," ESA, March 21(2012).

[19] Gabarró, C., J. Font, A. Camps, M. Vall-llossera, and A. Julià, "A new empirical model of the sea surface microwave emissivity for salinity remote sensing," Geophys. Res. Lett. 31, L01309, doi:10.1029/2003GL018964(2004).

[20] Durden, S. L., and J. F. Vesecky, "A physical radar crosssection model for a wind-driven sea with swell," IEEE J. Oceanic Eng.**10**(4), 445–451(1985).

[21] Schlitzer, R. "Ocean Data View," http://odv.awi.de, (2012).

[22] Boutin, J., Martin, N., Reverdin, G., Yin, X., and Gaillard, F., "Sea surface freshening inferred from SMOS and ARGO salinity:impact of rain," Ocean Sci. **9**, 183–192 (2013).

[23] NOAA Hurricane Center, "ISAAC Graphics Archive," 30 Aug.2012,http://www.nhc.noaa.gov/archive/2012/graphics/al09/loop_3W.shtml.